Evidence of the aerosol core-shell mixing state over Europe during the heat wave of summer 2003 by using CHIMERE simulations and AERONET inversions

Jean-Christophe Péré, Marc Mallet, Bertrand Bessagnet, Véronique Pont

Evidence of the aerosol core-shell mixing state over Europe during the heat wave of summer 2003 by using CHIMERE simulations and AERONET inversions

J. C. Péré,[1,2] M. Mallet,[2] B. Bessagnet,[1] and V. Pont[2]

Received 22 January 2009; revised 17 March 2009; accepted 10 April 2009; published 8 May 2009.

[1] The aim of this work consists to infer the most probable mixing state of aerosols over the European continent during the heat wave of summer 2003, where large concentrations of biomass burning and anthropogenic aerosols have been observed. The methodology presented here is based on the Single Scattering Albedo (SSA) sensitivity to the mixing state of particles. Three different mixing cases; external mixing, internal mixing, and core-shell type mixing have been considered. Composite SSA has been computed for this intense pollution event over Europe and are compared with the AErosol RObotic NETwork (AERONET) retrieved SSA values. The most probable mixing state seems to be core-shell mixing, with secondary aerosols coating over primary soot and mineral dust. This work underlines clearly that this specific representation should be used in modeling exercises for simulating anthropogenic and/or biomass burning direct and semi-direct aerosol effects and climate impact over the European region. **Citation:** Péré, J. C., M. Mallet, B. Bessagnet, and V. Pont (2009), Evidence of the aerosol core-shell mixing state over Europe during the heat wave of summer 2003 by using CHIMERE simulations and AERONET inversions, *Geophys. Res. Lett.*, *36*, L09807, doi:10.1029/2009GL037334.

1. Introduction

[2] Classically, two hypotheses could be used for treating aerosol mixing state in climate models. The most common approach is the external way, in which each particle consists of only one chemical substance. The other one consists in modeling aerosol optical properties by using the internal mixture (all particles contain a mixture of species from each of the sources), which could in turn be divided in two representations: the ''pure homogeneous'' and the ''core-shell'' one. The treatment of the mixing state of particles into climate models has crucial impacts [*Satheesh et al.*, 2006a, 2008] especially concerning black carbon (BC) aerosols as coating on BC particles can enhance their absorption of solar radiation [*Jacobson*, 2000; *Mikhailov et al.*, 2006], with large impacts on the semi-direct aerosol effect by modifying cloud properties and boundary layer evolution [*Ackerman et al.*, 2000; *Feingold et al.*, 2005].

[3] Up to now, most of global models describe aerosols as externally mixed although some recent works have shown that a core-shell treatment of particles should be more realistic, leading to significant differences in aerosol optical properties, compared to externally or internally homogeneous mixed states. *Jacobson* [1999] reported that for a model in which particles are treated in 'core shells' mixing approach agrees well with surface irradiance observations at Riverside and Claremont (USA). Over Asia, *Satheesh et al.* [2006b] reported that assuming aerosols in core-shells form (BC in shell and dust in core) improve considerably the comparisons between observed and simulated surface irradiances. *Chandra et al.* [2004] and *Dey et al.* [2008] have shown that over tropical Indian Ocean and during the summer monsoon season, model and observations agree well in cases of dust particles coated with BC.

[4] This work consists to infer the most probable mixing state of aerosols over the European continent by using an optical constrain [*Mallet et al.*, 2005]. The principle of this study is to compute aerosol column-averaged SSA from CHIMERE model simulations [*Bessagnet et al.*, 2004] for three different mixing states: internally homogeneous, core-shell and external and to compare them with SSA issued from AERONET retrievals [*Dubovik et al.*, 2000; *Holben et al.*, 1998]. This work is focused on the European region, where few studies about the treatment of the particle mixing have been conducted in spite of the presence of different aerosol species.

[5] We emphasize on the heat wave of summer 2003, corresponding to large concentrations of absorbing BC and secondary (sulfates, nitrates, secondary organics) aerosols over Europe. Such climate conditions observed during summer 2003 and associated with intense wildfires over the Mediterranean region are expected to become more frequent in a future warmer climate [*Moriondo et al.*, 2006].

2. CHIMERE Modeling

2.1. General Set-up

[6] In this study, a version of CHIMERE for a domain covering the western Europe is used: from 14°W to 28°E in longitude and from 35°N to 58.2°N in latitude, with a constant horizontal resolution of 0.4° × 0.4°. The vertical grid contains 15 layers from surface to 500 hPa. The aerosol module is that described in the work of *Bessagnet et al.* [2004]. The modeled species are sulfates, nitrates, ammonium, primary organic and black carbon, secondary organic aerosols, sea salt,, natural and anthropogenic dust and water. The gas-particle partitioning of the ensemble Sulfate/Nitrate/Ammonium is treated by the code ISORROPIA implemented in CHIMERE. Organic and BC emissions are issued from the *Junker and Liousse* [2008] study. Anthropogenic dust emissions are taken from EMEP inventory and

[1]Institut National de l'Environnement Industriel et des Risques, Verneuil-en-Halatte, France.
[2]Laboratoire d'Aérologie, Université de Toulouse, CNRS, Toulouse, France.

0094-8276/09/2009GL037334

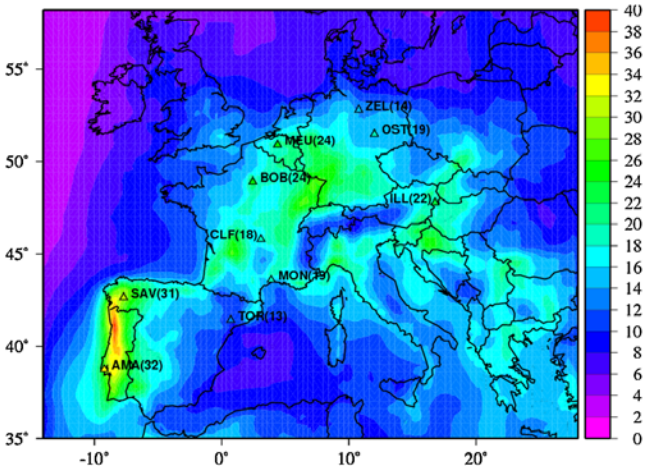

Figure 1. Time average over the first ten days of August 2003 of simulated PM2.5 ground mass concentrations ($\mu g/m^3$) and corresponding mean observed values at 10 AirBase sites (colored triangles): SAV, Savino (−7.70°E, 42.63°N); TOR, Torms (0.72°E, 41.40°N); AMA, Amadora (−9.21°E, 38.74°N); ILL, Illmitz (16.77°E, 47.77°N); CLF, Clermont-Ferrand (3.095°E, 45.78°N); ZEL, Zella-Mehlis (10.76°E, 52.80°N); MON, Montpellier (3.89°E, 43.59°N); BOB, Bobigny (2.45°E, 48.90°N); OST, Ost (12.01°E, 51.49°N); MEU, Meudon (4.39°E, 50.90°N).

natural dust are transported from boundary conditions calculated on a monthly base, and are locally produced within the domain after *Vautard et al.* [2005]. Fire emissions are taken into account and a detailed description of the emission dataset is given by *Hodzic et al.* [2007]. The MEGAN biogenic inventory was implemented in CHIMERE to estimate emissions of VOC and NO from vegetation. The particle size distribution ranges from about 40 nm to 10 μm and are distributed into 8 bins. Dynamical processes influencing aerosol population such as nucleation, coagulation, condensation/evaporation, adsorption/desorption, wet and dry deposition and scavenging are also taken into account.

2.2. Modeling of Aerosol Single Scattering Albedo

2.2.1. External Mixing

[7] In the external treatment, we consider that each particle consists of only one chemical substance. Here, we used the Mie code published by *Voshchinnikov* [2004] for calculating the extinction (Qext), scattering (Qscat) and absorption (Qabs) efficiency of a given species in each size bin. The overall simulated optical efficiencies are then the sum of the components aerosols ones [*Hess et al.*, 1998]. The real and imaginary part of the refractive index of each aerosol species used to perform our simulations are reported by *Mallet et al.* [2005].

2.2.2. Internally Homogeneous Mixing

[8] Here, we consider that the different aerosol species are "well-mixed" in each size bin. To reflect the chemical and optical average of all the contributing species, the refractive index is calculated from the refractive indexes of pure species by the volume weighting method [*Lesins et al.*, 2002]. Similarly, a mean particle density is determined. The extinction, scattering and absorption efficiencies of a single particle are calculated using the Mie theory for homogeneous sphere [*Voshchinnikov*, 2004]. The methodology developed by *Wu et al.* [1996] for a sectional aerosol distribution is then used to retrieve the optical properties of the total aerosol population.

2.2.3. Core-Shell Mixing

[9] The radiative module concerning the core-shell treatment is detailed in the work of *Mallet et al.* [2005]. Here, the extinction, scattering and absorption efficiencies of a single particle are computed with the n-layer spheres algorithm and the radiative properties of the total aerosol distribution by using the methodology of *Wu et al.* [1996]. In our simulations, primary aerosols (soot and mineral dust) are assumed to be the core. Here, "soot" is referenced as a mixture of BC and organic carbon [*Jacobson*, 2000]. Secondary particles (sulfates, nitrates, ammonium, secondary organic aerosols) and sea salt are assumed to be the shell material. The real and imaginary parts of the core and the shell have been determined using a volume average procedure [*Lesins et al.*, 2002].

3. Period of Simulation and AERONET Retrievals

[10] To infer the most probable mixing state of aerosols over European region, column-averaged SSA was computed from 1 July to 10 August 2003 over a domain covering western Europe for three different mixing cases and compared with AERONET retrieved SSA values.

[11] The meteorological conditions in July and the first half of August 2003 over Europe was characterized by the persistence of anticyclonic conditions and exceptionally high temperatures favorable to the accumulation of primary particulate matter and an important formation of secondary aerosols, which led to the development of a large scale pollution episode particularly intense during the first ten days of August 2003 [*Vautard et al.*, 2005]. Figure 1 shows mean PM2.5 surface concentrations simulated by CHIMERE and averaged over the first ten days of August 2003. In this figure, the wide extent of the pollution episode is clearly illustrated with mean PM2.5 surface concentrations ranging from 15 to 30 $\mu g/m^3$ over a large part of France, Benelux, Western Germany and Northern Italy and peaks reaching 40 $\mu g/m^3$ over Portugal where intense wildfires occurred during the heat wave of 2003 [*Hodzic et al.*, 2007]. For comparison with observed data, we use daily mean observations of PM2.5 from 10 background air quality monitoring sites located in Figure 1 (triangles). PM2.5 observations are fairly well estimated by the CHIMERE model with a mean underestimation in the range 10–25 % following the monitoring sites and an averaged one over the stations of 20 % mainly due to unidentified emission sources not accounted for in CHIMERE. However, with CHIMERE, concentrations of major aerosol species (nitrate, sulfate, ammonium and organic carbon) have been extensively validated in other studies [*Bessagnet et al.*, 2004; *Honoré et al.*, 2008]. Such important levels of pollution were higher than normally observed in summer [*Tressol et al.*, 2008] and were associated with high aerosol optical thickness over Europe [*Hodzic et al.*, 2007].

[12] For the summer 2003 period, level 2.0 and 1.5 (when level 2.0 was not available) SSA retrievals from 10 AERONET sites (Figure 3 and Table S1 of the auxiliary material) located as

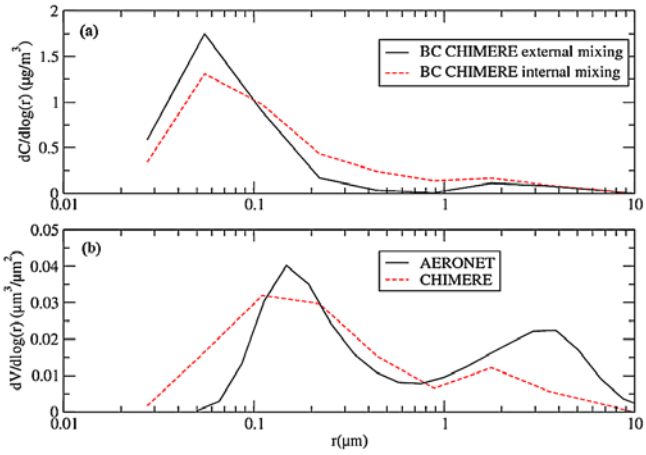

Figure 2. Time average between 1 July and 10 august 2003 at the site of Lille of (a) the simulated BC mass size distributions at the ground for the external and internal mixing and (b) the column volume size distribution of the total aerosol population simulated by CHIMERE (internal mixing) and retrieved by AERONET.

well close to as far from aerosol sources are considered.[1] The *Dubovik et al.* [2000] algorithm derives the aerosol size distribution and refractive index to calculate the AERONET SSA for the whole atmospheric column. In our study, we set the AERONET SSA uncertainty to ±0.04 by using only the data corresponding to aerosol optical thickness (at 440 nm) >0.2 [*Dubovik et al.*, 2000].

4. Results and Discussion

[13] The modeled column-averaged SSA (at 440nm) is calculated as follows:

$$SSA(440nm) = \sum_{k=0}^{k=nl} SSA_k(440nm) \times \left(\frac{AOT_k(440nm)}{AOT_{tot}(440nm)} \right)$$

where SSA_k and AOT_k are respectively the single scattering albedo and aerosol optical thickness of the layer k, AOT_{tot} is the aerosol optical thickness of the whole atmospheric column and nl is the number of model layer.

[14] Critical points in SSA calculations concern the (1) BC mass distribution, and (2) the choice of the BC refractive index. Figure 2 gives examples of simulated aerosol size distribution time-averaged between 1 July and 10 August of 2003 at Lille. Figure 2a displays simulated BC mass size distributions at the ground that are unimodal with a median radius r ∼ 0.05 μm for the external treatment and a larger one over the range 0.05–0.1 μm for the internal treatment due to coagulation and absorption processes between species. The obtained BC mass size distributions are found to be in agreement with those measured during the ESCOMPTE and POVA experiments by *Mallet et al.* [2003] and *Jaffrezo et al.* [2005]. In addition, the column volume size distribution for the total aerosol population simulated by CHIMERE (internal mixing case) is compared with AERONET retrievals. Two different modes in the accumulation (r ∼ 0.1–0.2 μm) and coarse (r > 1 μm) size range (Figure 2b) are simulated and fit well with AERONET retrievals.

[15] In a second time, sensitivity tests have been performed on the BC refractive index by using the values of 1.75–0.44i [*Hess et al.*, 1998] and 1.95–0.66i [*Bergström*, 1972]. The SSA calculated values are then compared with those obtained with the reference value of 1.87–0.569i [*Marley et al.*, 2001] used thereafter in our simulations (REF). These tests indicate discrepancies on the modeled SSA of ±0.01 for the external and core-shell aerosol mixing and ±0.02 for the internally homogeneous one. Moreover, in the absence of extensive validation of BC mass concentrations simulated by CHIMERE, we evaluated the impact of an increase/decrease of 20% of simulated BC mass concentrations on modeled SSA, showing a discrepancy of ±0.02 for the three aerosol mixing states. These two types of sensitivity tests indicate that one can reasonably consider cumulative uncertainties on modeled SSA of ±0.03 for the

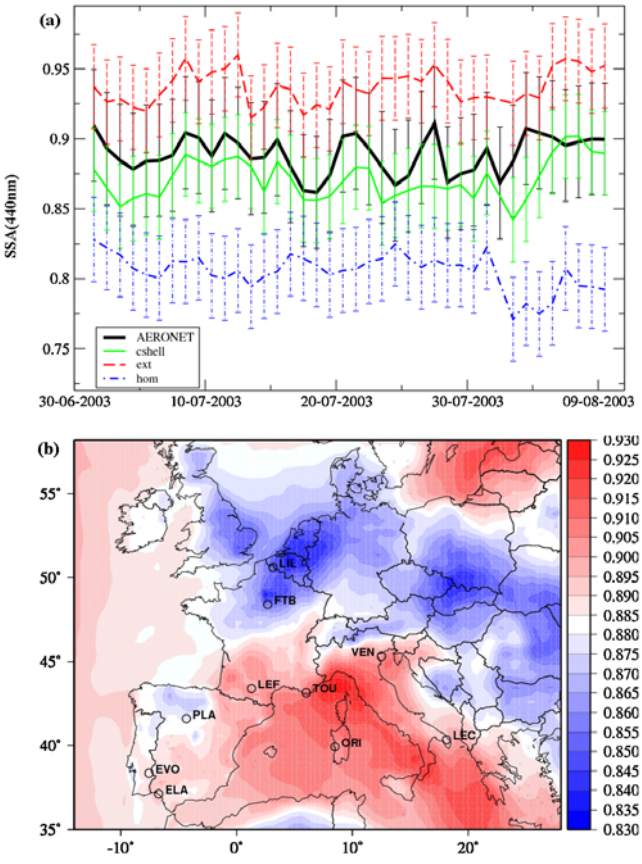

Figure 3. (a) Temporal evolution of daily mean SSA at 440 nm spatial-averaged over 10 AERONET sites from 1 July to 10 August 2003 for an aerosol external mixing (ext), internally homogeneous mixing (hom), core-shell mixing (cshell) along with corresponding AERONET observed values. The error bars represent the uncertainty range of observed (±0.04 [see *Dubovik et al.*, 2000]) and modeled (calculated from sensitivity tests described in section 4) SSA. (b) Time-averaged simulated SSA core-shell REF (at 440 nm) at the surface (SSA_{surf}) between 1 July and 10 August 2003 and locations of the 10 AERONET sites (circles).

[1]Auxiliary materials are available in the HTML. doi:10.1029/2009GL037334.

Table 1. Mean SSA at 440 nm Time-Averaged Between 1 July and 10 August 2003 and Spatial Averaged Over 10 AERONET Sites and Corresponding Spatio-temporal Correlation $R_{spatio\text{-}temp}$ for the Three Hypotheses on Aerosol Mixing State[a]

	Mean SSA(440nm)	$R_{spatio\text{-}temp}$
AERONET	0.90 ± 0.04	
External mixing	0.94 ± 0.03	0.35
Internally homogeneous mixing	0.80 ± 0.04	0.04
Core-shell mixing	0.89 ± 0.03	0.51

[a] $R_{spatio\text{-}temp}$ is the correlation calculated using the total number of SSA samples (N = 969) on the 10 AERONET sites for the whole study period (1 July to 10 August of 2003).

external and core-shell aerosol mixing and ±0.04 for the internally homogeneous one.

[16] Temporal evolution of daily mean modeled SSA at 440 nm spatial-averaged over the 10 AERONET sites from 1 July to 10 August 2003 for the three aerosol mixing cases along with AERONET observations are displayed in Figure 3a. Table 1 reports corresponding observed and modeled mean SSA values averaged over the period and spatio-temporal correlation $R_{spatio\text{-}temp}$. Figure 3a and Table 1 clearly show that the core-shell treatment has better ability to reproduce the spatio-temporal evolution of SSA over Europe during summer 2003 with a spatio-temporal correlation coefficient $R_{spatio\text{-}temp}$ of 0.51 (versus respectively 0.04 and 0.35 for the internally homogeneous and external treatment), and a mean value of 0.89 ± 0.03 close to the observed one (0.90 ± 0.04) (Table 1). This value corresponds to moderate absorbing aerosols and is consistent with observed value of 0.9 in July 2000 over north of France during the ESQUIF experiment [*Raut and Chazette*, 2008] and 0.87 < SSA < 0.91 over south eastern Spain during August 2003 [*Lyamani et al.*, 2006]. Figure 3a shows with no ambiguity important disagreement between model and AERONET concerning the two other approaches. Indeed, the internally homogeneous mixing is more sensitive to the choice of the BC complex refractive index and underestimates (0.80 ± 0.04) the mean observed SSA value. This low modeled value denotes a too much absorbing aerosol layer, which is consistent with previous findings showing that an homogeneous mixing of BC within less absorbing materials overestimates its absorption as more radiation interact with BC [*Jacobson*, 2000]. Moreover, the external approach overestimates (0.94 ± 0.03) the AERONET mean SSA value, denoting a too much reduction of particle absorption when BC is not internally-mixed; as shown by *Jacobson* [2000] and *Chandra et al.* [2004]. Furthermore, statistical comparisons of observed and modeled SSA (see Table S1 of the auxiliary material) clearly show that the core-shell mixing results are in better agreement with AERONET values with smaller biases (−4.57% < N-bias < 1.81%), compared to external and internally homogeneous approaches which result, respectively, in larger positive (2.24% < N-bias < 8.96 %) and larger negative (−15.75% < N-bias < −5.36%) biases.

[17] Spatial distribution of SSA core-shell REF (at 440 nm) at the surface (SSA_{surf}), time-averaged between 1 July and 10 August 2003, is displayed in Figure 3b. Different areas clearly appear reflecting the type of aerosol sources, with a decrease of SSA_{surf} over northern Spain and Portugal, related to absorbing biomass burning aerosols emitted by intense wildfires during summer 2003 [*Hodzic et al.*, 2007]. Similarly, the decrease of SSA_{surf} in northern France and Benelux regions reflects the accumulation of anthropogenic absorbing aerosols (high BC concentrations) in these high urbanized and industrialized areas. Moreover, important concentrations of scattering biogenic aerosols over the Massif Central region and scattering anthropogenic aerosols (high sulfates concentrations) in northern Italy (Pô Valley) (Figure 1) result in high values of modeled SSA_{surf} in these areas.

5. Conclusion

[18] Three different mixing scenarios of aerosols are tested during the intense heat wave of summer 2003 over Europe characterized by large concentrations of biomass burning and urban/industrial aerosols. Column-averaged simulated SSA is compared with the AERONET retrieved SSA, revealing clearly that primary aerosols (soot and mineral dust) coated with secondary species as treated by the core-shell method stands for as the most probable mixing state of aerosols over Europe. Indeed, the mean modeled core-shell SSA (0.89 ± 0.03) is close to the observed one (0.90 ± 0.04). The external and ''pure'' internally homogeneous approaches result respectively in higher (0.94 ± 0.03) and lower (0.80 ± 0.04) mean modeled SSA as compared to AERONET.

[19] **Acknowledgments.** We thank N. Voshchinnikov for providing the Mie code and efforts of PIs of the 10 AERONET sites used in this work. We would also like to acknowledge H. Chepfer and L. Menut at IPSL-LMD, CNRS, and A. Hodzic at NCAR for their scientific support.

References

Ackerman, A. S., et al. (2000), Reduction of tropical cloudiness by soot, *Science*, *288*, 1042–1047.

Bergström, R. W. (1972), Predictions of the spectral absorption and extinction coefficients of an urban air pollution model, *Atmos. Environ.*, *6*, 247–258.

Bessagnet, B., et al. (2004), Aerosol modeling with CHIMERE—Preliminary evaluation at the continental scale, *Atmos. Environ.*, *38*, 2803–2817.

Chandra, S., S. K. Satheesh, and J. Srinivasan (2004), Can the state of mixing of black carbon aerosols explain the mystery of 'excess' atmospheric absorption?, *Geophys. Res. Lett.*, *31*, L19109, doi:10.1029/2004GL020662.

Dey, S., S. N. Tripathi, and S. K. Mishra (2008), Probable mixing state of aerosols in the Indo-Gangetic Basin, northern India, *Geophys. Res. Lett.*, *35*, L03808, doi:10.1029/2007GL032622.

Dubovik, O., A. Smirnov, B. Holben, M. King, Y. Kaufman, T. Eck, and I. Slutsker (2000), Accuracy assessments of aerosol optical properties retrieved from Aerosol Robotic Network (AERONET) Sun and sky radiance measurements, *J. Geophys. Res.*, *105*, 9791–9806.

Feingold, G., H. Jiang, and J. Y. Harrington (2005), On smoke suppression of clouds in Amazonia, *Geophys. Res. Lett.*, *32*, L02804, doi:10.1029/2004GL021369.

Hess, M., P. Koepke, and I. Schult (1998), Optical properties of aerosols and clouds: The software package OPAC, *Bull. Am. Meteorol. Soc.*, *79*, 831–844.

Hodzic, A., S. Madronich, B. Bohn, S. Massie, L. Menut, and C. Wiedinmyer (2007), Wildfire particulate matter in Europe during summer 2003: Meso-scale modeling of smoke emissions, transport and radiative effects, *Atmos. Chem. Phys.*, *7*, 4043–4064.

Holben, B. N., et al. (1998), AERONET: A federated instrument network and data archive for aerosol characterization, *Remote Sens. Environ.*, *66*, 1–16.

Honoré, C., et al. (2008), Predictability of European air quality: Assessment of 3 years of operational forecasts and analyses by the PREV'AIR system, *J. Geophys. Res.*, *113*, D04301, doi:10.1029/2007JD008761.

Jacobson, M. (1999), Isolating nitrated and aromatic aerosols and nitrated aromatic gases as sources of ultraviolet light absorption, *J. Geophys. Res.*, *104*, 3527–3542.

Jacobson, M. (2000), A physically-based treatment of elemental carbon optics: Implications for global direct forcing of aerosols, *Geophys. Res. Lett.*, *27*, 217–220.

Jaffrezo, J.-L., G. Aymoz, and J. Cozic (2005), Size distribution of EC and OC in the aerosol of Alpine valleys during summer and winter, *Atmos. Chem. Phys.*, *5*, 2915–2925.

Junker, C., and C. Liousse (2008), A global emission inventory of carbonaceous aerosol from historic record of fossil fuel and biofuel consumption for the period 1860–1997, *Atmos. Chem. Phys.*, *8*, 1195–1207.

Lesins, G., P. Chylek, and U. Lohmann (2002), A study of internal and external mixing scenarios and its effect on aerosol optical properties and direct radiative forcing, *J. Geophys. Res.*, *107*(D10), 4094, doi:10.1029/2001JD000973.

Lyamani, H., F. J. Olmo, A. Alcantara, and L. Alados-Arboledas (2006), Atmospheric aerosols during the 2003 heat wave in southeastern Spain II: Microphysical columnar properties and radiative forcing, *Atmos. Environ.*, *40*, 6465–6476.

Mallet, M., J. C. Roger, S. Despiau, O. Dubovik, and J.-P. Putaud (2003), Microphysical and optical properties of aerosol particles in urban zone during ESCOMPTE, *Atmos. Res.*, *69*, 73–97.

Mallet, M., V. Pont, and C. Liousse (2005), Modelling of strong heterogeneities in aerosol single scattering albedos over a polluted region, *Geophys. Res. Lett.*, *32*, L09807, doi:10.1029/2005GL022680.

Marley, N. A., et al. (2001), An empirical method for the determination of the complex refractive index of size- fractionated atmospheric aerosols for radiative transfer calculations, *Aerosol Sci. Technol.*, *34*, 535–549.

Mikhailov, E. F., S. S. Vlasenko, I. A. Podgorny, V. Ramanathan, and C. E. Corrigan (2006), Optical properties of soot–water drop agglomerates: An experimental study, *J. Geophys. Res.*, *111*, D07209, doi:10.1029/2005JD006389.

Moriondo, M., P. Good, R. Durao, M. Bindi, C. Gianakopoulos, and J. Corte-Real (2006), Potential impact of climate change on fire risk in the Mediterranean area, *Clim. Res.*, *31*, 85–95.

Raut, J. C., and P. Chazette (2008), Vertical profiles of urban aerosol complex refractive index in the frame of ESQUIF airborne measurements, *Atmos. Chem. Phys.*, *8*, 901–919.

Satheesh, S. K., J. Srinivasan, V. Vinoj, and S. Chandra (2006a), New directions: How representative are aerosol radiative impact assessments?, *Atmos. Environ.*, *40*, 3008–3010.

Satheesh, S. K., J. Srinivasan, and K. K. Moorthy (2006b), Spatial and temporal heterogeneity in aerosol properties and radiative forcing over Bay of Bengal: Sources and role of aerosol transport, *J. Geophys. Res.*, *111*, D08202, doi:10.1029/2005JD006374.

Satheesh, S. K., K. Krishna Moorthy, S. Suresh Babu, V. Vinoj, and C. B. S. Dutt (2008), Climate implications of large warming by elevated aerosol over India, *Geophys. Res. Lett.*, *35*, L19809, doi:10.1029/2008GL034944.

Tressol, M., et al. (2008), Air pollution during the 2003 European heat wave as seen by MOZAIC airliners, *Atmos. Chem. Phys.*, *8*, 2133–2150.

Vautard, R., B. Bessagnet, M. Chin, and L. Menut (2005), On the contribution of natural Aeolian sources to small particle concentrations in Europe, testing hypotheses with a modeling approach, *Atmos. Environ.*, *39*, 3291–3303.

Voshchinnikov, N. V. (2004), Optics of cosmic dust, *Astrophys. Space Phys. Rev.*, *12*, 1–182.

Wu, X., C. Seigneur, and R. Bergstrom (1996), Evaluation of a sectional representation of size distributions for calculating aerosol optical properties, *J. Geophys. Res.*, *101*, 19,277–19,283.

B. Bessagnet and J. C. Péré, Institut National de l'Environnement Industriel et des Risques, Parc Technologique ALATA BP 2, F-60550 Verneuil-en-Halatte CEDEX, France. (jean-christophe.pere@ineris.fr)

M. Mallet and V. Pont, Laboratoire d'Aérologie, Université de Toulouse, CNRS, 14 avenue Edouard Belin, F-31400 Toulouse CEDEX, France.